

# Nonlinear Characteristics of Ventricular Fibrillation Depend on Myocardial Infarction Locations

María González-González<sup>1</sup>, Óscar Barquero-Pérez<sup>1</sup>, Cristina Soguero-Ruiz<sup>1</sup>,  
Juan José Sánchez-Muñoz<sup>2</sup>, José Luis Rojo-Álvarez<sup>1</sup>, Arcadi García-Alberola<sup>2</sup>

<sup>1</sup>Department of Signal Theory and Communications, University Rey Juan Carlos, Madrid, Spain

<sup>2</sup>Unit of Arrhythmias, Hospital Universitario Virgen de la Arrixaca, Murcia, Spain

## Abstract

*The location of the myocardial infarction (MI) might induce a change in the characteristics of cardioelectric signals recorded during ventricular fibrillation (VF). In the literature, spectral analysis has been used to characterize VF, however, spectral parameters do not account for nonlinear information on these signals.*

*The aim of this work was to analyze the effect of the location of the infarcted area on VF signals by using nonlinear parameters, hence complementing their spectral characterization. We included patients with chronic MI (28 anterior, 29 inferior) from Hospital Universitario Virgen de la Arrixaca (Murcia) and Hospital Universitario Gregorio Marañón (Madrid) in Spain. VF was induced during cardioverter defibrillator implant. We computed the following spectral parameters: dominant frequency ( $f_d$ ), organization index ( $oi$ ), and regularity index ( $ri$ ). We also computed the following nonlinear indices: sample entropy ( $SampEn$ ), and higher order moments, kurtosis ( $K$ ) and skewness ( $S$ ).*

*Statistical differences between Anterior and Inferior MI patients was assessed by a hypothesis tests based on bootstrap resampling. None of the spectral measures showed significant differences between Anterior and Inferior groups. However, all of the nonlinear indices were significantly different.  $SampEn$  was higher in Inferior MI patients, whereas  $K$  and  $S$  were lower in Anterior MI patients. Nonlinear and higher order moments indices ( $SampEn$ ,  $K$  and  $S$ ) showed significant differences during VF depending on the MI localization. Therefore, nonlinear indices might help to complement spectral indices characterizing VF signals.*

## 1. Introduction

Ventricular fibrillation (VF) is one of the major arrhythmias associated with cardiac arrest [1]. During VF the ventricles do not beat in a coordinated way, leading to in-

efficient beats, so that there is no cardiac output, leading rapidly to death.

Recently, features based on spectral analysis has been applied to characterize the VF signal [2, 3]. However, the mechanisms underlying the VF are not completely understood. Moreover, the highly disorganized, fragmentary nature of the VF cannot be completely characterized by means of spectral analysis. Even though, it has been proved that VF is not a chaotic process [4], some complexity and nonlinear measures might allow to gain a deeper understanding characterizing the VF.

The aim of this work is to describe the spectral and nonlinear characteristics of the electrical signal recorded by an intracardiac electrodes during induced VF in patients with chronic myocardial infarction (MI). We propose to assess nonlinear characteristics of VF signals by means of sample entropy ( $SampEn$ ) and high-order moments of the amplitude distributions using the kurtosis and the skewness. We aim, also, to evaluate the effect of the location of the infarcted area on VF spectral and nonlinear features by means of a bootstrap statistical analysis.

The structure of the paper is as follows. In Section 2 the VF signal preprocessing, spectral analysis, and nonlinear VF analysis methods are described. In Section 3 the database is described. In Section 4 the statistical analysis of the data is detailed. In Section 5 the results are presented, and finally in Section 6 conclusions and future work are presented.

## 2. Methods

### 2.1. VF signal processing and spectral analysis

The onset of each VF episode was manually annotated, and the following 3 seconds were selected. We decided to analyze 3 seconds because this period of time was adequate to estimate the spectrum of the signal according to the sampling frequency and the spectral band of interest.

The signal preprocessing consisted in a wander baseline cancellation using a 250-ms median filter and spline interpolation [5].

Spectrum was estimated for each EGM segment using a Welch periodogram, with Hamming window of 128 samples, and 50% overlap, and spectral resolution of 1.024 samples. We computed the following indices from the spectrum estimation:

*Dominant frequency* ( $f_d$ ) defined as the frequency at which the absolute spectral maximum occurs.

*Regularity index* ( $ri$ ) defined as the ratio of the power in a 75% bandwidth around the  $f_d$ , to the power of the [3, 15] Hz band [6].

*Organization index* ( $oi$ ) defined as the ratio between the total power in the frequency band [3, 30] Hz and the power in a 75% bandwidth for the spectral peaks corresponding to the fundamental frequency  $f_d$  and to every harmonic within this band [7].

## 2.2. Nonlinear VF analysis

Entropy-based methods provide a quantification of the irregularity of a temporal series. Among them, *SampEn* [8], which is a modification of the Approximate Entropy [9], holds some properties that are appropriate for the study of physiological signals. The *SampEn* is the negative natural logarithm of the conditional probability that two sequences which are similar for  $m$  points remain similar for  $m + 1$  points. Thus, a lower value of *SampEn* indicates more self-similarity in the time series. In order to compute the *SampEn*, the specification of two parameters is previously required, namely, the embedded dimension  $m$ , that is, the length of the vectors to be compared, and a noise filter threshold  $r$ .

The procedure for *SampEn* calculation given a time series with  $N$  data points is as follows

- $B_i^m(r)$  is defined as  $(N - m - 1)^{-1}$  times the number of template vectors  $\mathbf{x}_m(j)$  similar to  $\mathbf{x}_m(i)$  (within  $r$ ) where  $j = 1 \dots N - m$  with  $j \neq i$ .
- The average of  $B_i^m(r)$  for all  $i$  is calculated as

$$B^m(r) = \frac{1}{N - m} \sum_{i=1}^{N-m} B_i^m(r)$$

- Similarly  $A_i^m(r)$  is defined as  $(N - m - 1)^{-1}$  times the number of template vectors  $\mathbf{x}_{m+1}(j)$  similar to  $\mathbf{x}_{m+1}(i)$  (within  $r$ ) where  $j = 1 \dots N - m$  with  $j \neq i$ .
- The average of  $A_i^m(r)$  for all  $i$  is calculated as

$$A^m(r) = \frac{1}{N - m} \sum_{i=1}^{N-m} A_i^m(r)$$

- *SampEn*( $m, r$ ) and its statistic *SampEn*( $m, r, N$ ) are defined

as follows

$$SampEn(m, r) = \lim_{N \rightarrow \infty} \{-\ln [A^m(r)/B^m(r)]\}$$

$$SampEn(m, r, N) = -\ln [A^m(r)/B^m(r)]$$

*SampEn* is robust to noise and outliers, hence it has been widely applied to characterize the HRV signal [10].

We characterize high-order moments of the VF signals by means of the *skewness* and the *kurtosis*. Specifically, we want to characterize the symmetry (skewness) and the peakedness (kurtosis) of the distribution of amplitudes [11].

The sample skewness  $S$ , and kurtosis  $K$ , can be computed from the time series  $x[n]$ ;  $n = 1, \dots, N$ , where  $N$  is the number of samples of the time series, as:

$$S = \frac{\left(\frac{1}{N} \sum_{i=1}^N x[i] - \mu\right)^3}{\sigma^3} \quad (1)$$

$$K = \frac{\left(\frac{1}{N} \sum_{i=1}^N x[i] - \mu\right)^4}{\sigma^4} \quad (2)$$

where  $\mu$  is the sample mean and  $\sigma$  is the sample standard deviation.

A time series with the same number of larger and smaller values than the mean has skewness zero ( $S = SGauss = 0$ ), which is the case for Gaussian distributed amplitude values. Usually complex time series have fluctuations that are not Gaussian distributed [12]. So that, time series with many smaller values than the mean (and few larger values) have positive skewness ( $S > SGauss = 0$ ). Whereas a time series with many larger values than the mean (and few smaller) have negative skewness ( $S < SGauss = 0$ ). A time series with many values near the mean value has a kurtosis greater than 3 ( $K > KGauss = 3$ ), therefore the distribution of amplitudes is sharper than a Gaussian. Figure 1 (bottom) shows an example of the probability density function estimation, and  $K$  and  $S$  values computed on VF electrogram (EGM) signals from a patients with Anterior and Inferior MI.

## 3. Data

Consecutive patients with chronic MI > 3 months old undergoing an implantable cardioverter defibrillator (ICD) implant for clinical reasons between November 2001 and August 2003 in two tertiary hospitals were included in this retrospective study. The implant protocol at the time of the study required the induction of at least two consecutive VF episodes in order to ensure a safety margin for defibrillation. The ICD was programmed to record intracardiac EGMs during VF in a pseudounipolar configuration using

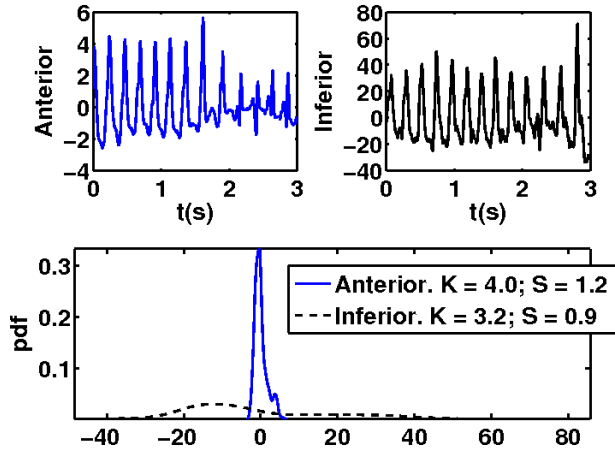


Figure 1. (top) Two VF EGM signals examples from patients with Anterior and Inferior MI. (bottom) Probability density function of amplitude distribution of the VF EGM signals.  $K$  and  $S$  are different for Anterior and Inferior MI patients.

the defibrillation *coil* in the right ventricle and the *can* the indifferent electrode. The recorded EGMs were saved in digital format (128 samples per second) for further analysis.

61 patients were included in the study, 29 with anterior MI (47.5% group A), and 32 with inferior MI (52.5%, group B). Age ( $63.0 \pm 9.9$  years for group A and  $65.2 \pm 8.6$  years for group B) and gender (one female in each group) were not significantly different between groups.

#### 4. Statistical analysis

To test whether exists statistically significant differences on spectral and nonlinear indices between Anterior and Inferior MI patients we performed statistical hypothesis tests based on bootstrap resampling. The null hypothesis ( $H_0$ ) represents no difference between Anterior and Inferior MI patients, against the alternative hypothesis ( $H_1$ ) that there exists significant differences. We used the mean difference between each indices computed on Anterior and Inferior groups as the statistic to summarize our data. Bootstrap hypothesis test is based on the idea of building an empirical distribution of the statistic, under  $H_0$ , and then computing the statistic on  $B$  different resamplings. Assuming that  $H_0$  is true, bootstrap statistics are computed on resamplings from a population which is the concatenation of the indices from Anterior and Inferior groups. We computed p-value as the fraction of the points on the distribution (probability) that are more extreme than the actual statistic value [13, 14].

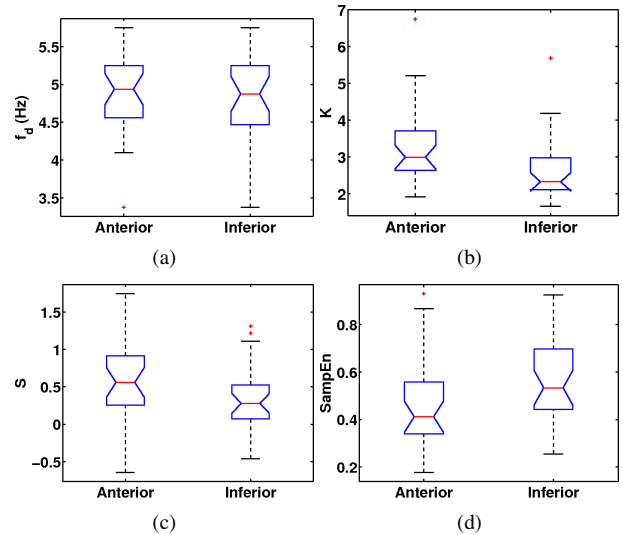


Figure 2. Boxplots.

#### 5. Results

Table 1 shows the mean and standard deviation values for each index. Statistically significant differences between Anterior and Inferior MI patients are highlighted. Figure 2 shows boxplots for  $f_d$  and nonlinear indices ( $K$ , and  $S$ ,  $SampEn$ ).

None of the spectral indices ( $f_d$ ,  $ri$ , and  $oi$ ) was significantly different between Anterior and Inferior MI patients. In contrast, all nonlinear indices were significantly different. In patients with Inferior MI,  $SampEn$  was significantly higher ( $0.47 \pm 0.20$  vs  $0.57 \pm 0.17$ ), therefore the complexity of VF EGM signals was higher on Inferior than on Anterior MI patients. Higher order moments were also significantly different. Indeed,  $K$  was higher than 3 in patients with Anterior MI and lower than 3 in patients with Inferior MI. These results points out that patients with Anterior MI had more sample values at the mean and in the tails than a normal distribution. The behaviour was the opposite ( $K < 3$ ) in patients with Inferior MI.

The asymmetry of the amplitudes distributions,  $S$ , was also significantly different between Inferior and Anterior MI patients. In both groups the  $S$  was higher than 0, therefore with positive skewness.

#### 6. Conclusions

The nonlinear characteristics of intracardiac signals during VF depend on the MI location. More complex (irregular) VF signals is seen in Inferior MI patients. Also, distribution of signal amplitudes are more concentrated around the mean (high values of  $K$ ) in Anterior MI patients, exhibiting also a high positive skewness of the distribution. Overall, these results should be taken into account when

	Anterior	Inferior	<i>p</i> - value
<i>f<sub>a</sub></i> (Hz)	4.85 ± 0.52	4.83 ± 0.52	n.s.
<i>r<sub>i</sub></i>	0.79 ± 0.12	0.82 ± 0.10	n.s.
<i>o<sub>i</sub></i>	0.83 ± 0.10	0.82 ± 0.10	n.s.
<b>SampEn</b>	<b>0.47 ± 0.20</b>	<b>0.57 ± 0.17</b>	<b>p &lt; 0.05</b>
<b>K</b>	<b>3.32 ± 0.15</b>	<b>2.71 ± 0.89</b>	<b>p &lt; 0.05</b>
<b>S</b>	<b>0.62 ± 0.61</b>	<b>0.34 ± 0.41</b>	<b>p &lt; 0.05</b>

Table 1. Mean ± standard deviation of spectral and non-linear indices on AMI and IMI patients. *p* - value < 0.05 is considered a statistical significant difference.

analyzing further clinical studies involving patients with infarctions in terms of spectral features of their presenting arrhythmias.

Spectral characteristics analyzed in this work did not show any difference. This result is in agreement with results in [2]. The differences between Anterior and Inferior MI patients may be due to an alteration of the electrophysiologic properties of the myocardium induced by the infarcted area and does not necessarily reflect different intrinsic characteristics of the VF. Several experimental studies have shown that the existence of an infarcted area may change the frequency content of local EGMs during VF, hence leading to changes in the complexity of the signal and in the distribution of amplitudes.

Our results suggest that patients with Inferior MI show a higher complexity in VF signals. Inferior MIs can involve the right ventricle and might be closer to the ICD recording electrode than anterior infarcts, potentially explaining the obtained results. In contrast, a larger amount of electrically active myocardium would be expected in the inferior infarct group, since Anterior MIs are more often associated with extensive scars. More precise information on the size and location of the infarcted areas as well as their anatomic relationship with the electrode position might be obtained with image techniques and could be useful to better assess this issue, but we lack this information due to the retrospective character of the study. A second limitation derives from the use of an ICD to obtain the EGMs, which reduces the available signal to a unique intracardiac recording. Multiple recordings from both ventricular chambers during sinus rhythm and VF might be useful to further delineate the influence of the MI location and size on the spectral characteristics of the arrhythmia.

## Acknowledgments

This work was partially supported by Research Project TEC2010-19263 (Spanish Government). Authors OBP and CSR have the support of FPU Grants AP2009-1726 and FPU12/04225 from the Ministerio de Educación, Spanish Government.

## References

- [1] Goldberger AL. Clinical Electrocardiography: A Simplified Approach. Mosby, 1994.
- [2] Sánchez Muñoz JJ, Rojo-Álvarez JL, García-Alberola A, et al. Effects of the location of myocardial infarction on the spectral characteristics of ventricular fibrillation. Pacing and clinical electrophysiology PACE 2008;31(6):660–665.
- [3] Barquero-Pérez O, Rojo-Álvarez JL, Caamaño AJ, Goya-Esteban R, et al. Fundamental frequency and regularity of cardiac electrograms with Fourier organization analysis. IEEE transactions on bio medical engineering 2010; 57(9):2168–2177.
- [4] Kaplan DT, Cohen RJ. Is fibrillation chaos? Circulation Research 1990;67(4):886–892.
- [5] Sörnmo L, Laguna P. Bioelectrical signal processing in cardiac and neurological applications. Academic Press, 2005.
- [6] Sanders P. Spectral Analysis Identifies Sites of High-Frequency Activity Maintaining Atrial Fibrillation in Humans. Circulation 2005;112(6):789–797.
- [7] Everett TH, Kok LC, Vaughn RH, Moorman JR, Haines DE. Frequency domain algorithm for quantifying atrial fibrillation organization to increase defibrillation efficacy. IEEE transactions on bio medical engineering 2001; 48(9):969–978.
- [8] Richman JS, Moorman JR. Physiological time-series analysis using approximate entropy and sample entropy. American Journal of Physiology Heart and Circulatory Physiology 2000;278(6):H2039–H2049.
- [9] Pincus SM. Approximate entropy as a measure of system complexity. Proceedings of the National Academy of Sciences of the United States of America 1991;88(6):2297–2301.
- [10] Goya-Esteban R, Sandberg F, Barquero-Pérez O, García-Alberola A, Sörnmo L, Rojo-Álvarez JL. Seven-day Analysis of Atrial Fibrillation and Circadian Rhythms. Bio inspired System and Signal Processing 2013;1(1):20–24.
- [11] Peña D. Fundamentos de Estadística. Alianza Editorial, 2008.
- [12] Cristelli M, Zaccaria A, Pietronero L. Universal relation between skewness and kurtosis in complex dynamics. Physical Review E 2012;85(6):066108.
- [13] Efron B, Tibshirani RJ. An Introduction to the Bootstrap. Chapman and Hall, 1994.
- [14] Kaplan D. Resampling Stats in Matlab. Resampling Stats. Inc., Arlington, VA, 1999.

Address for correspondence:

O Barquero-Pérez

Department of Signal Theory and Communications

University Rey Juan Carlos. B104, Camino del Molino s/n  
28943 - Fuenlabrada (Madrid), Spain

Phone: +34 91 488 84 62

oscar.barquero@urjc.es